Available online at www.CivileJournal.org

# Civil Engineering Journal

Vol. 5, No. 8, August, 2019


# Major Parameters Affect the Non-Liner Response of Structure Under Near-Fault Earthquakes

Ali A. Muhsin [a*], Hussam K. Risan [a]

[a] *Civil Engineering Department, Al-Nahrain University, Baghdad, 10072, Iraq.*

Received 30 March 2019; Accepted 03 July 2019

**Abstract**

Near-fault ground motion can be identified by the presence of a predominant long duration pulse in the velocity traces mainly due to directivity effect. This pulse exposes the structure to high input energy at the beginning of the earthquake which leads to a higher response in comparison with the ordinary ground motions. This paper investigates 79 earthquake records with different properties to achieve three goals: the first aim is to compare between the linear and nonlinear response of SDOF systems under near-fault and far-fault earthquakes. While the second objective is to examine the parameters that control the characteristics of near-fault earthquakes. Two factors have been studied which is PGV/PGA ratio and pulse period. Finally, the seismic code provisions related to the near-fault earthquakes were evaluated in term of the elastic acceleration response spectrum, the evaluation is adopted for American Society of Civil Engineers code ASCE 7 and Uniform Building Code UBC. The results lead to the following conclusions: with respect to a specific PGA, the near-fault earthquake imposed higher response in comparison with far-field earthquakes. The near-fault earthquakes become severe as the PGV/PGA and pulse period increase. The interested seismic codes can cover the actual behavior based on the average response of a certain amount of data, while it may become non-conservative relative to an individual record.

*Keywords:* Near-Fault Earthquake; Pulse Period; PGV/PGA; Strength Reduction Factor; Response Spectrum.

## 1. Introduction

Near-field earthquake identified by limited frequency and high amplitude pulse with a long duration that may or may not appear in the acceleration time history but it is significantly obvious in the velocity traces. This kind of ground motions put the structures under high input energy at the starting of earthquake due to the effect of two phenomena called directivity effect and fling step effect. The directivity effect occurs when the fault rapture travels toward the site at a velocity very close to the shear wave velocity. This will expose the structures to high amplitude with long duration pulse that extremely affects the structural response. Conversely, the backward directivity effect happens when the fault spread apart from the site, such effect can produce a long duration ground motion traces with small amplitude [1]. On the other hand, the fling step effect takes place when the two sides of the fault moved relative to each other. This movement happened in a manner that causes permanent displacement on the tectonic plate which leads to one side pulse in the velocity time history and step pulse in the displacement traces [2].

Due to the special properties of the near-fault earthquakes, it deserves a deeper discussion to clarify all the mysterious points related to this phenomenon. Many conclusions regard the structural response under near-fault earthquakes have been discussed in previous attempts. Chopra and Chintanapakdee (2001) diagnosed the changes in the spectral regions

* Corresponding author: aliabdulwahid80@gmail.com

http://dx.doi.org/10.28991/cej-2019-03091365

due to near-fault effect. It is pointed out that, in case of near-fault motions, the acceleration and displacement sensitive regions become much wider while the velocity sensitive region becomes narrower in comparison with far-fault motions. This effect increases the range of structures that respond in a stiff manner under near-fault earthquakes [3]. The linear and nonlinear response of frame buildings that subjected to the near-fault earthquake is studied by Alavi and Krawinkler (2004) [4]. The results showed that, for a structure with a period longer than pulse period, the yielding starts at high stories, however as the base shear strength drop, the ductility demands shift to the bottom stories. While for a structure with a period less than pulse period, a large ductility demand always occurs in the lower stories. Furthermore, the difference in response of shear wall building under near-fault and far-fault motions is illustrated by Heydari and Mousavi (2015) [5]. It is observed that the relative displacement due to near-field records is twice that obtained from far-field records. Additionally, the relative displacement of the building under the near-field effect increases as the ratio of the structural period to the pulse period becomes larger.

Alhan and Sürmeli (2015) examined the validity of near-source factors that adopted in the UBC code by studying the response of 3, 8 and 15 story building subjected to near-field ground motions. It is concluded that the provisions of seismic codes without near-source factors underestimate the behavior of the buildings [6]. However, the examined near-source factors need more modifications to produce a better response estimation. Hosseini et al. (2017) discussed the suitability of the seismic code provisions that should ensure life safety performance level for the reinforced concrete buildings under near-fault earthquakes. Three-component nonlinear time history analysis conducted for a set of buildings. He found that the performance of some cases reached beyond the life safety level and some of them even collapsed. So it is concluded that the code requirements need to be improved and consider the high intensity of the vertical ground motion component in the near-source earthquakes [7]. Talebi Jouneghani et al. (2017) points out that the linear response of high-frequency structures to near-fault earthquakes is less than nonlinear behavior of the same buildings, since that the near-fault ground motions have low-frequency content and the nonlinearity decreases the frequency of the structure [8]. Kohrangi et al. (2018) investigate how the shape of the acceleration response spectrum for pulse-like motions affects the response of the buildings. By examining a set of earthquakes with and without pulse-like which has equivalent acceleration response spectrum shapes. He noticed that the severity of the near-fault earthquakes cannot be predicted only by the shape of the spectrum and it's important to investigate deeply the pulse properties which have the major effect on the intensity of the ground motion [9].

It is noted that the previous attempts are dealing with a relatively limited number of ground motions to investigate a specific case study which normally leads to conditional results. Hence it is important to perform comprehensive investigation including a wide range of near-fault earthquakes that has different characteristics such as fault mechanism, site condition, PGA and magnitude. This paper investigates 79 earthquake records with different properties to achieve the following topics: discussing the response of elastic and inelastic SDOF systems under near-fault and far-fault excitations. Investigating the effect of pulse period and PGV/PGA on the response of SDOF systems. Assessing the seismic code provision with regard to near-fault earthquakes based on elastic response spectrum. An overview of the steps of the research methodology can be seen in Figure 1.

## 2. Selected Ground Motions

A set of 79 earthquakes was selected from pacific earthquake engineering research center (PEER) ground motion database [10], including 74 near-fault and 5 far-fault ground motions. The magnitudes of near-fault earthquakes range from 5 to 7.6 with the closest distance to the fault plane, not more than 30 km. These earthquakes are classified as pulse-like ground motion according to a technical report for PEER ground motion database [11]. On the other hand, the selected far-fault earthquakes namely without pulse, have a magnitude range from 5.7 to 7.28 and located at a distance not less than 87 km from the fault plane. Tables 1 and 2 show the details of selected near-field and far-field earthquakes respectively.

## 3. Software Analysis

The Dynamic analysis is conducted by Prism version 1.0.2 which is a seismic analysis application dealing with only single degree of freedom systems and can perform the following functions: modifying the earthquake records, adopting the Newmark integration method to conducting the time history analysis by employing a several type of hysteresis patterns, and also, the ability of determining the elastic and inelastic response spectrum. The results of Prism software are verified with the results obtained by Sap2000. Both programs produce identical results in linear and nonlinear states.

The examined SDOF system has a range of vibration periods starting from 0.02 sec and limited by 10 sec with step 0.02 sec, all these vibration periods chosen under 5% damping ratio. The material nonlinearity is represented by the variety of the stiffness. While the damping is assumed to be constant through elastic and inelastic stages. The bi-linear hysteric model is adopted to represent the nonlinear behavior, in which the post to pre-yielding stiffness ratio set to zero. Whereas the ductility factor, defined as the ratio of the maximum inelastic displacement to yield displacement, selected to be 2.

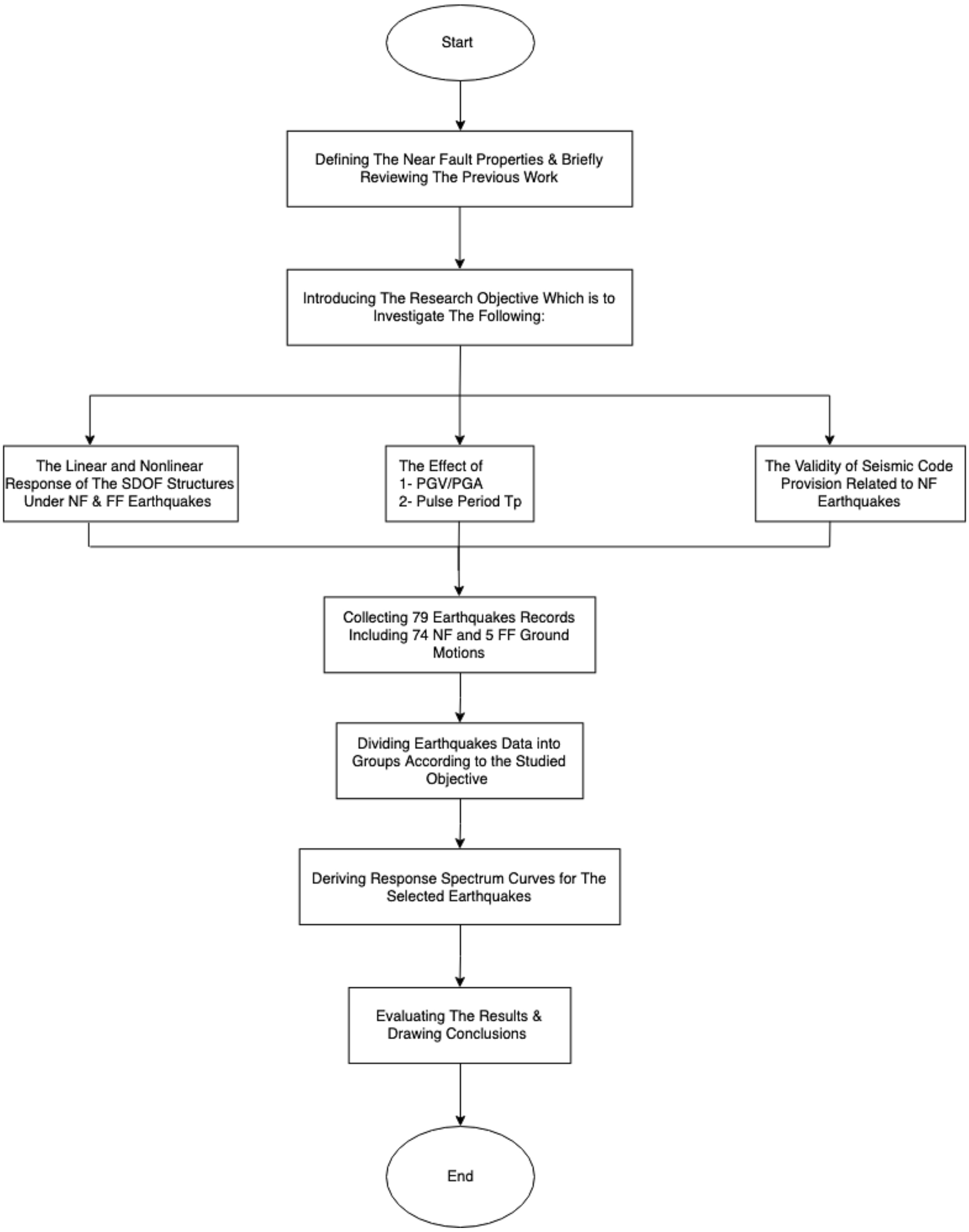


**Figure 1. Flowchart of research methodology**

**Table 1. Near fault earthquakes**

| Earthquake | Station | M[1] | $R_{rup}$[2] km | PGV/PGA sec | $T_p$[3] Sec |
|---|---|---|---|---|---|
| San Fernando, US | Pacoima Dam (upper left abut) | 6.6 | 01.8 | 0.10 | 01.6 |
| Coyote Lake, US | Gilroy Array #6 | 5.7 | 03.1 | 0.11 | 01.2 |
| Imperial Valley-06, US | Aeropuerto Mexicali | 6.5 | 00.3 | 0.14 | 02.4 |
| Imperial Valley-06, US | Agrarias | 6.5 | 00.7 | 0.22 | 02.3 |
| Imperial Valley-06, US | Brawley Airport | 6.5 | 10.4 | 0.23 | 04.0 |
| Imperial Valley-06, US | EC County Center FF | 6.5 | 07.3 | 0.32 | 04.5 |
| Imperial Valley-06, US | El Centro - Meloland Geot. Array | 6.5 | 00.1 | 0.32 | 03.3 |
| Imperial Valley-06, US | El Centro Array #10 | 6.5 | 06.2 | 0.30 | 04.5 |
| Imperial Valley-06, US | El Centro Array #11 | 6.5 | 12.5 | 0.12 | 07.4 |
| Imperial Valley-06, US | El Centro Array #3 | 6.5 | 12.9 | 0.18 | 05.2 |

| | | | | | |
|---|---|---|---|---|---|
| Imperial Valley-06, US | El Centro Array #4 | 6.5 | 07.1 | 0.22 | 04.6 |
| Imperial Valley-06, US | El Centro Array #5 | 6.5 | 04.0 | 0.26 | 04.0 |
| Imperial Valley-06, US | El Centro Array #6 | 6.5 | 01.4 | 0.26 | 03.8 |
| Imperial Valley-06, US | El Centro Array #7 | 6.5 | 00.6 | 0.25 | 04.2 |
| Imperial Valley-06, US | El Centro Array #8 | 6.5 | 03.9 | 0.11 | 05.4 |
| Imperial Valley-06, US | El Centro Differential Array | 6.5 | 05.1 | 0.22 | 05.9 |
| Imperial Valley-06, US | Holtville Post Office | 6.5 | 07.7 | 0.24 | 04.8 |
| Mammoth Lakes-06, US | Long Valley Dam (Upr L Abut) | 5.9 | 16.2 | 0.08 | 01.1 |
| Irpinia, Italy | Sturno (STN) | 6.9 | 10.8 | 0.23 | 03.1 |
| Westmorland, US | Parachute Test Site | 5.9 | 16.7 | 0.24 | 03.6 |
| Coalinga-05, US | Oil City | 5.8 | 08.5 | 0.05 | 00.7 |
| Coalinga-05, US | Transmitter Hill | 5.8 | 09.5 | 0.06 | 00.9 |
| Coalinga-07, US | Coalinga-14th & Elm (Old CHP) | 5.2 | 11.0 | 0.05 | 00.4 |
| Morgan Hill, US | Coyote Lake Dam (SW Abut) | 6.2 | 00.5 | 0.06 | 01.0 |
| Morgan Hill, US | Gilroy Array #6 | 6.2 | 09.9 | 0.13 | 01.2 |
| N. Palm Springs, US | North Palm Springs | 6.1 | 04.0 | 0.10 | 01.4 |
| San Salvador | Geotech Investig Center | 5.8 | 06.3 | 0.12 | 00.9 |
| Whittier Narrows-01,US | Downey - Co Maint Bldg | 6.0 | 20.8 | 0.16 | 00.8 |
| Whittier Narrows-01,US | LB - Orange Ave | 6.0 | 24.5 | 0.14 | 01.0 |
| Superstition Hills-02,US | El Centro Imp. Co. Cent | 6.5 | 18.2 | 0.16 | 02.4 |
| Superstition Hills-02,US | Parachute Test Site | 6.5 | 01.0 | 0.32 | 02.3 |
| Loma Prieta, US | Gilroy - Gavilan Coll. | 6.9 | 10.0 | 0.09 | 01.8 |
| Loma Prieta, US | Gilroy Array #1 | 6.9 | 09.6 | 0.07 | 01.2 |
| Loma Prieta, US | Gilroy Array #2 | 6.9 | 11.1 | 0.13 | 01.7 |
| Loma Prieta, US | Gilroy Array #3 | 6.9 | 12.8 | 0.13 | 01.5 |
| Loma Prieta, US | LGPC | 6.9 | 03.9 | 0.17 | 03.0 |
| Loma Prieta, US | Saratoga - Aloha Ave | 6.9 | 08.5 | 0.14 | 04.5 |
| Loma Prieta, US | Saratoga - W Valley Coll. | 6.9 | 09.3 | 0.20 | 01.9 |
| Erzican, Turkey | Erzincan | 6.7 | 04.4 | 0.28 | 02.7 |
| Cape Mendocino, US | Petrolia | 7.0 | 08.2 | 0.14 | 03.0 |
| Landers, US | Lucerne | 7.3 | 02.2 | 0.19 | 05.1 |
| Landers, US | Yermo Fire Station | 7.3 | 23.6 | 0.21 | 07.5 |
| Northridge-01, US | LA Dam | 6.7 | 05.9 | 0.15 | 01.7 |
| Northridge-01, US | Newhall - Fire Sta | 6.7 | 05.9 | 0.17 | 02.2 |
| Northridge-01, US | Newhall - W Pico Canyon Rd. | 6.7 | 05.5 | 0.29 | 02.4 |
| Northridge-01, US | Pacoima Dam (downstr) | 6.7 | 07.0 | 0.11 | 00.5 |
| Northridge-01, US | Pacoima Dam (upper left) | 6.7 | 07.0 | 0.08 | 00.9 |
| Kocaeli, Turkey | Yarimca | 7.5 | 04.8 | 0.31 | 04.5 |
| Chi-Chi, Taiwan | CHY035 | 7.6 | 12.7 | 0.18 | 01.4 |
| Chi-Chi, Taiwan | CHY101 | 7.6 | 10.0 | 0.28 | 04.8 |
| Chi-Chi, Taiwan | TCU029 | 7.6 | 28.1 | 0.27 | 06.4 |
| Chi-Chi, Taiwan | TCU036 | 7.6 | 19.8 | 0.43 | 05.4 |
| Chi-Chi, Taiwan | TCU038 | 7.6 | 25.4 | 0.40 | 07.0 |
| Chi-Chi, Taiwan | TCU040 | 7.6 | 22.1 | 0.39 | 06.3 |
| Chi-Chi, Taiwan | TCU042 | 7.6 | 26.3 | 0.15 | 09.1 |
| Chi-Chi, Taiwan | TCU052 | 7.6 | 00.7 | 0.39 | 08.5 |
| Chi-Chi, Taiwan | TCU053 | 7.6 | 06.0 | 0.35 | 13.0 |
| Chi-Chi, Taiwan | TCU054 | 7.6 | 05.3 | 0.22 | 10.0 |
| Chi-Chi, Taiwan | TCU056 | 7.6 | 10.5 | 0.28 | 13.0 |
| Chi-Chi, Taiwan | TCU065 | 7.6 | 00.6 | 0.16 | 05.7 |

| | | | | | |
|---|---|---|---|---|---|
| Chi-Chi, Taiwan | TCU068 | 7.6 | 00.3 | 0.73 | 12.0 |
| Chi-Chi, Taiwan | TCU075 | 7.6 | 00.9 | 0.34 | 05.1 |
| Chi-Chi, Taiwan | TCU076 | 7.6 | 02.8 | 0.15 | 04.0 |
| Chi-Chi, Taiwan | TCU082 | 7.6 | 05.2 | 0.25 | 09.2 |
| Chi-Chi, Taiwan | TCU087 | 7.6 | 07.0 | 0.38 | 09.0 |
| Chi-Chi, Taiwan | TCU102 | 7.6 | 01.5 | 0.31 | 09.7 |
| Chi-Chi, Taiwan | TCU103 | 7.6 | 06.1 | 0.56 | 08.3 |
| Chi-Chi, Taiwan | TCU104 | 7.6 | 12.9 | 0.55 | 12.0 |
| Chi-Chi, Taiwan | TCU128 | 7.6 | 13.2 | 0.45 | 09.0 |
| Chi-Chi, Taiwan | TCU136 | 7.6 | 08.3 | 0.27 | 10.0 |
| Yountville, US | Napa Fire Station #3 | 5.0 | 11.5 | 0.10 | 00.7 |
| Chi-Chi, Taiwan-03 | CHY024 | 6.2 | 19.7 | 0.18 | 03.2 |
| Chi-Chi, Taiwan-03 | CHY080 | 6.2 | 22.4 | 0.15 | 01.4 |
| Chi-Chi, Taiwan-03 | TCU076 | 6.2 | 14.7 | 0.11 | 00.9 |

$M^1$: Earthquake moment magnitude

$R_{rup}^2$: Closest distance to the fault plane

$T_p^3$: Pulse period

**Table 2. Far fault earthquakes**

| Earthquake | Station | M | $R_{rup}$, km | PGV, mm/sec | PGA, g |
|---|---|---|---|---|---|
| Gulf of California, US | El Centro Array #7 | 5.70 | 100.55 | 011 | 0.02 |
| Chi-Chi, Taiwan | TCU045 | 6.20 | 077.38 | 012 | 0.01 |
| San Fernando, US | Anza Post Office | 6.61 | 173.16 | 023 | 0.04 |
| Northridge, US | Hemet - Ryan Airfield | 6.69 | 144.71 | 047 | 0.05 |
| Landers, US | Baker Fire Station | 7.28 | 087.94 | 110 | 0.11 |

## 4. Linear Response

Earthquake spectrum response can illustrate a comprehensive understanding of the structural behavior with a wide range of vibration periods. Since that each point on the response spectrum curves represents a peak response of the SDOF structure with associated vibration period. This advantage is employed to compare near-fault with far-fault earthquakes in term of the displacement, velocity and acceleration response spectra. To simplify the presentation of results, only five near-fault earthquakes were chosen to compare with the mean response spectrum of the five far-fault earthquakes as shown in Figure 2. All records considered in this research were normalized to satisfy PGA equal to 30% of the gravity acceleration (0.3g).

Figure 2 shows that near-fault earthquakes create a larger response with considerable difference in displacement and velocity spectra while the difference tends to reduce in the acceleration spectra. This gives evidence that the acceleration response spectrum cannot accurately measure the severity of the pulse-like ground motions so that the response spectrum analysis should be avoided and more detailed analysis such as time history is preferable in case of design building to near-fault earthquakes. To demonstrate the obtained results, two relations should be highlighted here [12]:

$$E_{max} = \frac{1}{2}\, k\, {S_d}^2{}_{max} \quad (1)$$

$$V_{max} = k\, S_{d_{max}} \quad (2)$$

Where $E_{max}$ is the maximum strain energy, $k$ is the stiffness of the SDOF structure, $S_d$ is the displacement response spectrum and $V_{max}$ is the maximum base shear force.

Equations 1 and 2 imply that the displacement response spectrum can clearly quantify the maximum strain energy stored in the structure and the maximum base shear hits the structure during the earthquake. Hence after monitoring Figure 1, it is can be noticed that near-fault earthquakes subject the structure to high input energy and produce a higher strength demand in comparison with the far-fault earthquakes. One more point should be mentioned here, that in spite of both near-fault and far-fault excitations have similar PGA, the response of the elastic SDOF systems exhibit larger demands in near-fault case relative to far-fault one. That means, the severity of earthquakes was poorly measured by the PGA, and the structural response is sensitive to the pattern of acceleration variation with time.

## 5. Nonlinear Response

The strength reduction factor R, defined as the ratio between the strength required to keep the system in the elastic range $F_o$ to the yield strength of the system $F_y$ ($R = F_o/F_y$), is used to quantify the strength demand of the inelastic SDOF systems. The value of R is equal to unity in the linear SDOF system and it is greater than 1 in the nonlinear range, which mean that when the strength reduction factor of a structure has a small value beyond the unity, the structure requires a high yielding strength to withstand the earthquake and vice versa.

The SDOF systems are exposed to normalize near fault-and far-fault excitation produced by Chi Chi and Landers earthquakes respectively. Figure 3 illustrates the variation of the strength reduction factor R with respect to the period of vibration T of elastic perfectly plastic SDOF systems with ductility factor of 2 under near-fault and far-fault ground motions. It is observed that the strength reduction factor of the near-fault record is less than far-fault which means that for the same PGA and ductility demands the near-fault excitation produce a larger strength demand. Moreover, the strength reduction factor tends to be 1 at very short periods which implies that in spite of the considered ductility factor, there is no reduction in the design strength, while at very long periods the strength reduction factor approaches the value of ductility factor 2. Accordingly, if the long periods structures permitted to undergo through inelastic behavior, then the design strength is significantly reduced corresponding to the selected ductility factor.

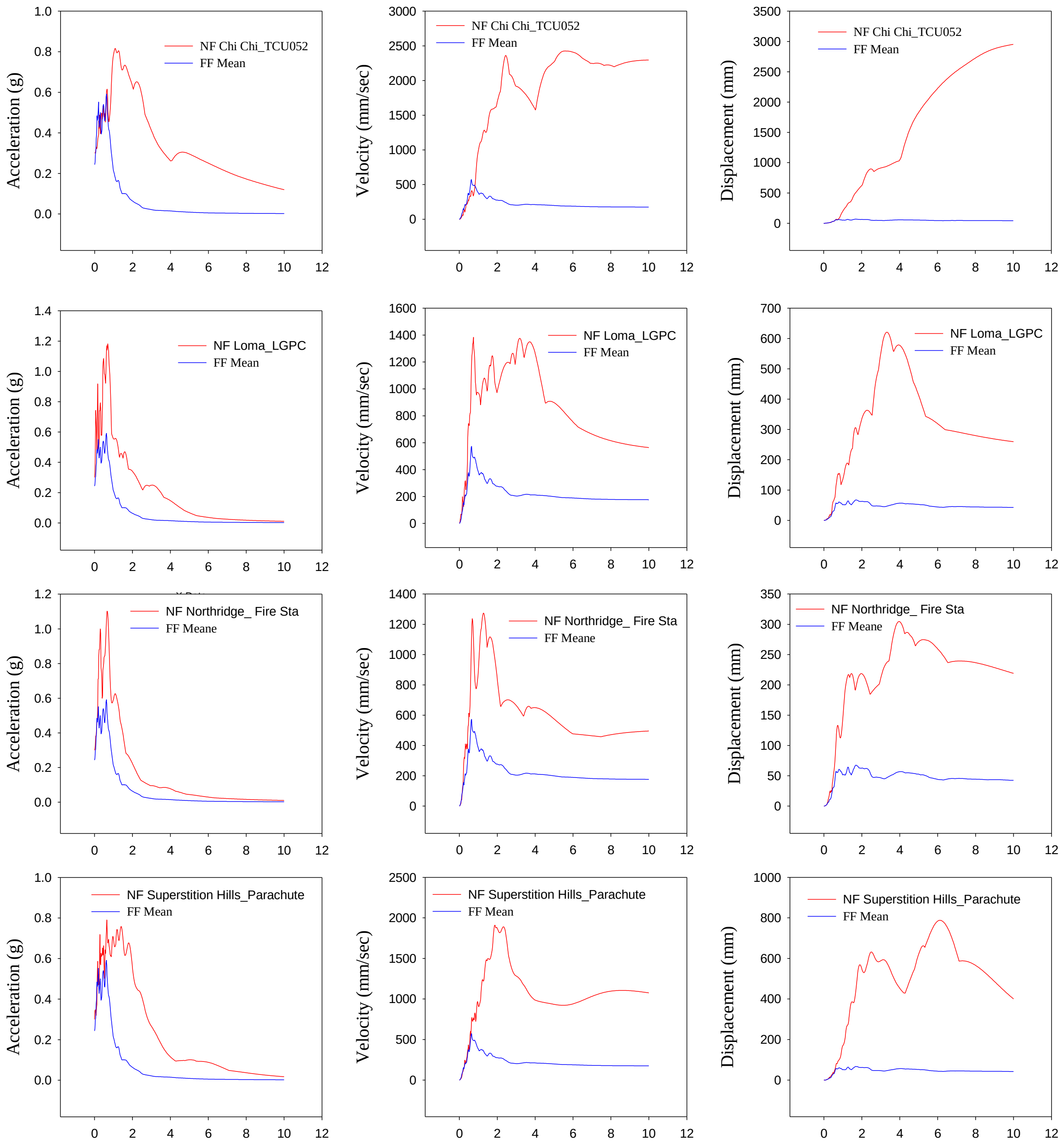

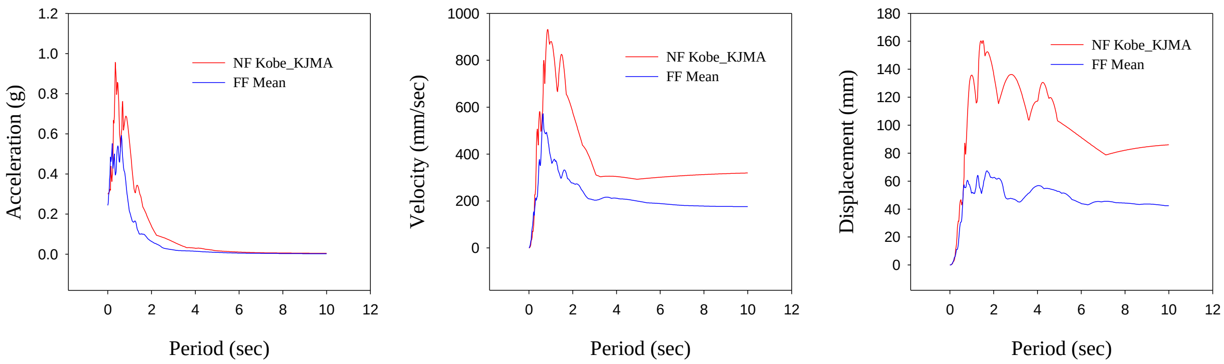


**Figure 2. Comparison between the near-field and far-field earthquakes in term of acceleration, velocity and displacement response spectra**

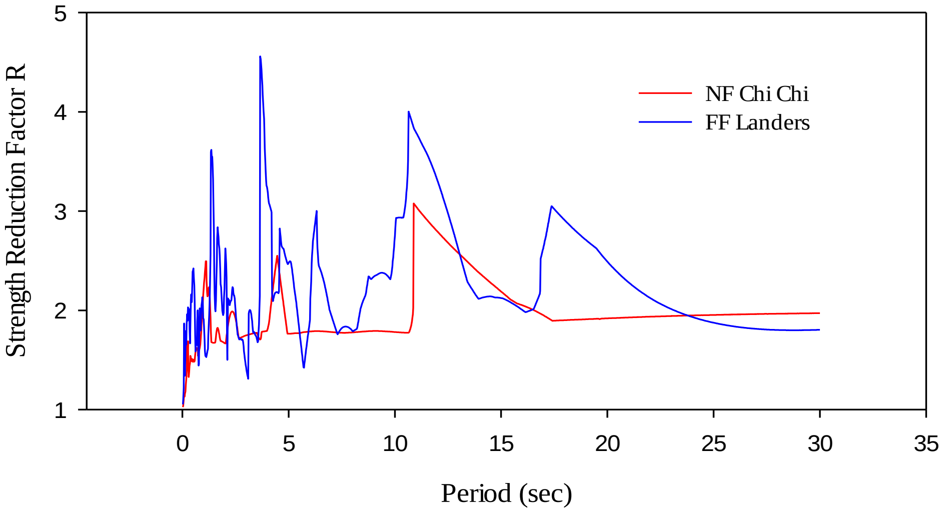


**Figure 3. Strength reduction factor vs. period of vibration for near-fault Chi Chi and far-fault Landers earthquakes under constant ductility factor of 2**

## 6. The Effect of PGV/PGA Ratio

Near-fault motions imposed a relatively high ratio of PGV to PGA, due to the distinct velocity pulse associated with such kind of motions. To investigate the effect of this ratio on the response of inelastic SDOF systems, the set of 74 near-fault earthquakes presented in Table 1 are divided into two groups, the first one with PGV/PGA < 0.2 and the second one with PGV/PGA > 0.2 knowing that each set contains 37 ground motion records. These earthquakes are used to study the response of elastic perfectly plastic SDOF systems with ductility factor of 2. Figure 4 shows the mean inelastic displacement against the vibration periods for the two groups of studied earthquakes. It is noted that short period systems insensitive to the variation of PGV/PGA ratio, on the other hand, the long vibration period structures exhibit a significantly larger displacement corresponding to higher PGV/PGA ratio. This results in line with that obtained by Liao et al. (2001) when he examined the effect of PGV/PGA ratio on two buildings with vibration periods 0.78 sec and 1.4 sec where the longest period building exhibit a larger story drift as the PGV/PGA ratio increase [13]. Conversely, the shorter period buildings not much affected by increasing the PGV/PGA ratio.

## 7. The Effect of Pulse Period

To discuss how the period of coherent velocity pulse impacts the behavior of the structures, four near-fault earthquakes with different pulse periods (Tp) were selected and examined in term of the inelastic displacement spectrum with ductility factor equal to 2.

The selected earthquakes are Coyote Lake, station Gilroy Array #6; Imperial Valley, station El Centro Array #6, station El Centro Array #8 and Landers, Yermo Fire Station, and their pulse periods are 1.2, 3.8, 5.4 and 7.5 sec respectively. Figure 5 shows the inelastic displacement response spectrum for selected earthquakes.

It is observed that the spectrum has a bell shape around the pulse periods which mean that the inelastic displacement demands increased as the vibration period of the structure approaches the pulse period. So it is essential to keep the vibration periods of the designed structure as far as possible from the pulse periods of the design earthquake to avoid high response demand. For a comprehensive study, more records need to be evaluated, for that the near-fault ground motions presented in Table 1 are assorted to three ranges of pulse periods: Tp< 2 sec, 2 < Tp< 5 sec, Tp > 5 sec. The mean inelastic displacement spectrum with ductility factor of 2 for the three ranges of pulse periods are illustrated in Figure 6. It is clear that the spectrum demand increases as the pulse periods become longer and the peck displacement demands occur around the pulse periods ranges.

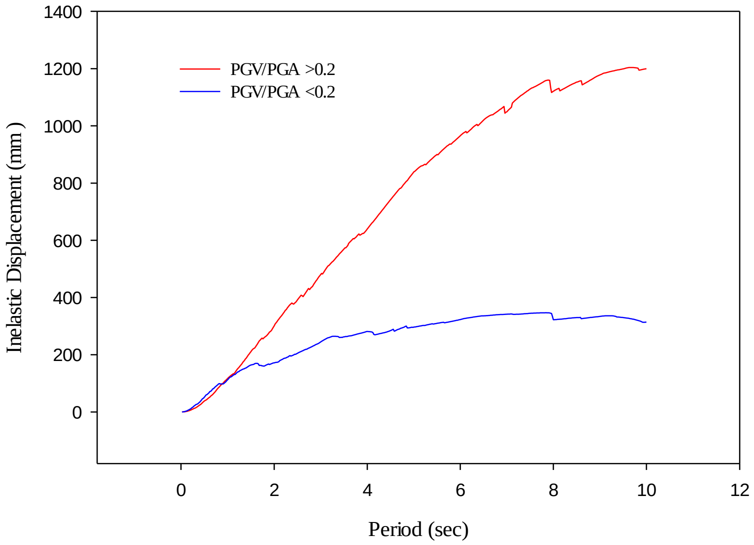


**Figure 4. The effect of PGV/PGA ratio of near fault earthquakes on the response of inelastic systems**

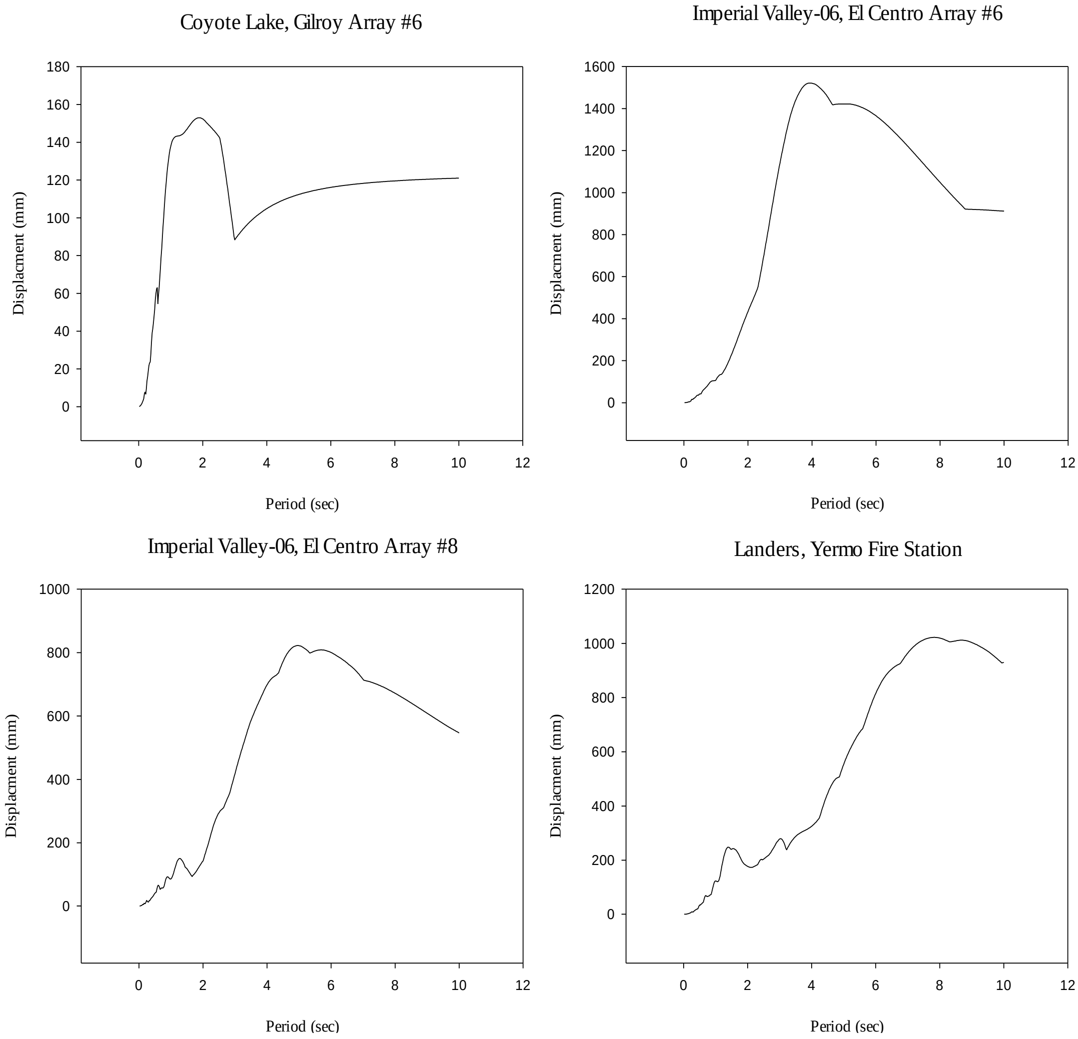


**Figure 5. The effect of pulse period on the inelastic displacement response spectra**

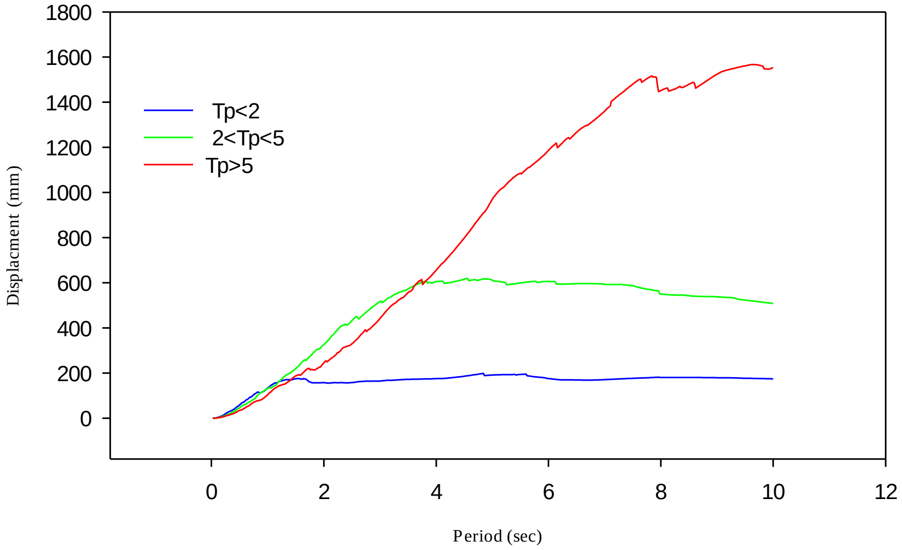


**Figure 6. The inelastic displacement response spectrum for three ranges of pulse period**

## 8. Comparison with Seismic Codes

Seismic codes aim to produce a structure which can adequately withstand the deformations and forces due to an earthquake. However, the provisions of these codes cannot totally prevent the damages, but it should protect the structures from collapse during the ground motions. The design response spectrum is an effective tool offered by seismic codes to predict the behavior of structures under seismic loads. Many factors should be considered to derive the shape and amplitude of the design response spectrum such as the magnitude of the earthquake, the shortest distance to the fault plane, the type of soil, and the importance of the structure. Depending on such parameters, each seismic code performed its own seismic hazard analysis to produce a smoothed design response spectrum which should satisfy the requirements of seismic design.

ASCE 7 [14], and UBC [15] codes were selected in this research to discuss the validity of the design response spectrum presented by these codes with respect to near-fault earthquakes. The ASCE 7 code presents two scales for the elastic design response spectrum: one depending on the maximum considered earthquake (MCE) which is rare event assumed to happen once each 2500 years, and the second depends on the design earthquake that occurs once each 500 years. These response spectra are derived with respect to three parameters: soil site class, risk category, and the spectral response acceleration parameters Ss and S1. The evaluating of these parameters entails three steps: first, a proper soil site class should be selected depending on the shear wave velocity at the top 30m of the soil profile. Where the ASCE 7 classified the soil to 6 classes from A to F starting from the strong soil (rock) to weak soil (soft clay). Secondly, the occupancy of the target structure should be specified to choose one of the four risk categories proposed by ASCE 7. Finally, Ss and S1 obtained from a contour map given within ASCE 7 which describe how the MCE affects the short period structures (0.2 sec.) and long-period structures (1 sec.) respectively.

The ASCE 7 code did not include the near-fault effects clearly in the derivation of the elastic response spectrum, the UBC considers that effect directly by suggesting near-source factors which applies to the area located near the active seismic source. In addition to the soil type, the elastic response spectrum in a near-fault region controlled by two other parameters: the closest distance to the known seismic source and the magnitude of the design earthquake. These factors used to amplify the seismic coefficients Ca and Cv which describe the elastic response spectrum. Since the response spectrum of UBC depending on the magnitude of the earthquakes, the near-fault records presented in Table 1 are classified into 3 boundaries according to the magnitude: $M \geq 7$, $6.5 \leq M < 7$, $M < 6.5$ which identified as group A, B, and C respectively. Then each group is compared with the associated response spectrum proposed by UBC. On the other hand, the ASCE 7 used to compare with 45 near-fault motions that occurred in the United State that implicitly presented Table 1.

Figure 7 presents the elastic response spectrum of UBC with respect to the mean spectrum of the corresponding near-fault record group. The mean plus standard deviation spectrum is also included to indicate how much the average difference of the records from the mean value.

According to the examined data, it is observed that the mean spectrum in harmony with that of UBC, except the spectrum of group A where the response of long duration periods (longer than 4 sec) is underestimated by UBC spectrum. However, the mean plus standard deviation spectrum considerably higher than code spectrum, this difference is observed at the long periods in group A and at the amplitude of the spectrum in group B and C. The maximum difference has an amplification value of 1.88, 1.65 and 1.86 for group A, B and C respectively.

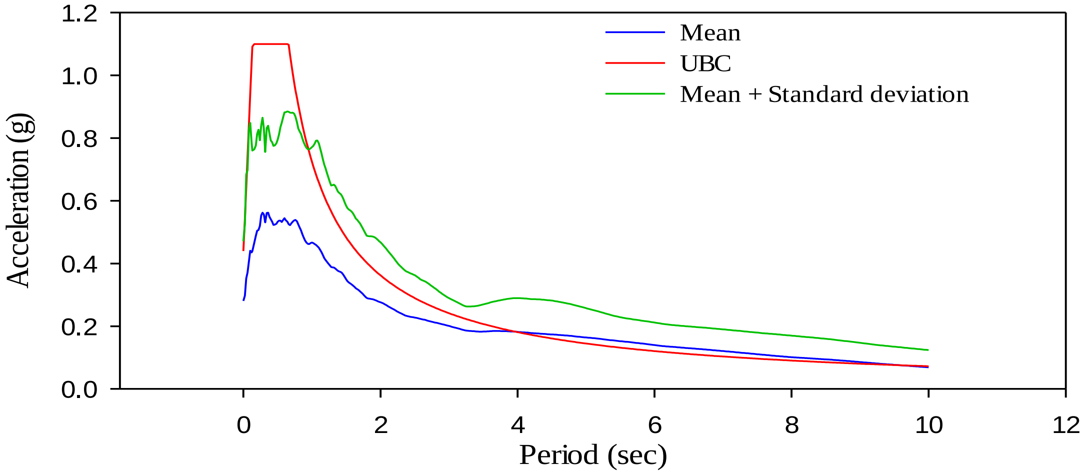


(a) Group A ( M ≥ 7 )

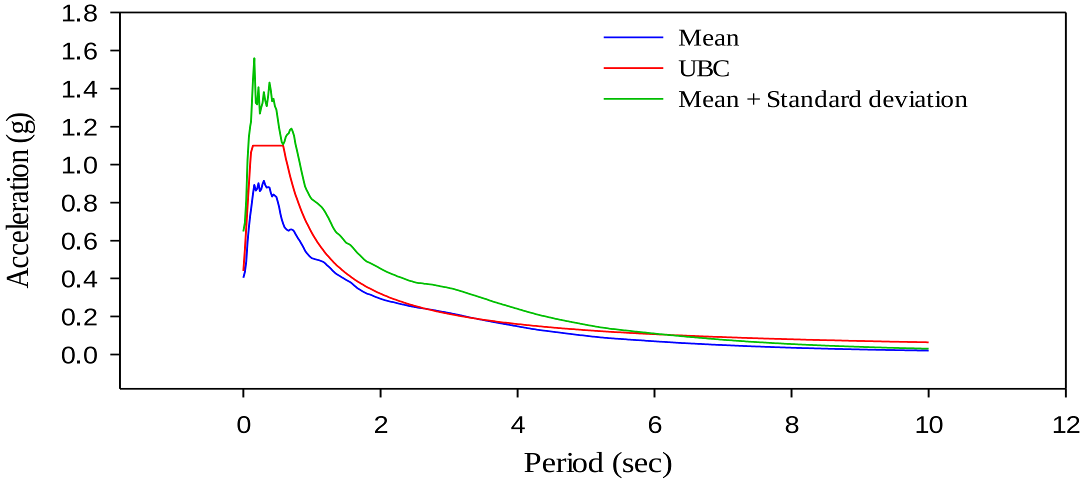


(b) Group B ( 6.5 ≤ M < 7 )

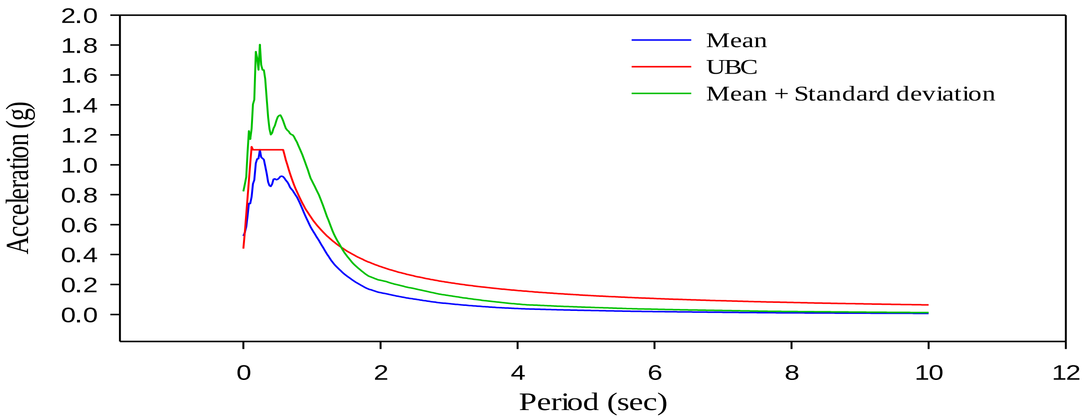


(c) Group C (M < 6.5)

**Figure 7. Elastic response spectrum of UBC code in comparison with mean spectrum of (a) group A, (b) group B, (c) group C.**

Figure 8 shows the evaluation of ASCE 7 elastic spectrum relative to the mean spectrum of associated earthquakes. In spite of that, ASCE 7 doesn't consider the near-source factors, it has covered the average response spectrum of the examined set of records exceedingly. Once more the mean plus standard deviation spectrum introduces a response higher than the code spectrum with a maximum difference of 1.4 at the short period range. It is concluded that the examined seismic codes spectrum may underestimate the structural response with respect to the individual near-fault earthquakes while it can catch the mean response if several records were considered. This is reasonable because the seismic codes produce the shape and the amplitude of the spectrum depending on a wide range of data.

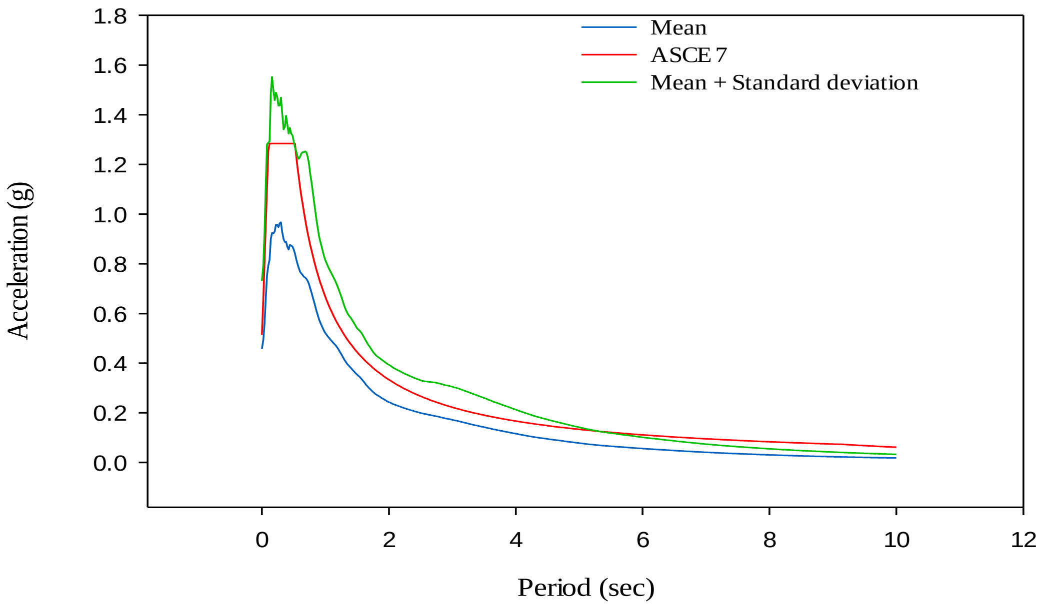


**Figure 8. Elastic response spectrum of ASCE 7 code in comparison with mean spectrum**

## 9. Conclusions

This study examined the behavior of elastic and inelastic SDOF systems under a range of near-fault and far-fault ground motions with different characteristics to get comprehensive results that may be used to predict the response of the multi-degree of freedom structure which has the same vibration period. It is noted that the previous attempts are dealing with a relatively limited number of ground motions to investigate a specific case study which normally leads to conditional results. Hence it is important to perform comprehensive investigation including a wide range of near-fault earthquakes that has different characteristics such as fault mechanism, site condition, PGA and magnitude. In this paper, we investigated 79 earthquake records with different properties. The dynamic analysis results lead to the following conclusions:

- The large displacement response spectrum of the near-fault earthquakes indicates that such kind of ground motions subject the structure to high input energy and produce a high strength demand in comparison with the far-fault earthquakes.
- The acceleration response spectrum cannot accurately measure the severity of the pulse-like ground motions so that the response spectrum analysis should be avoided and more detailed analysis such as time history is preferable in case of design building to near-fault earthquakes.
- The PGA is an inaccurate measurement of the earthquake's intensity. Where the near-fault ground motions produce a higher response in comparison with the far-fault motions for a similar value of PGA.
- It is observed that for the identical PGA value and same ductility demands, the near-fault excitation produces a larger strength demand relative to ordinary earthquakes.
- The strength reduction factor of the very short period structures (stiff structures) tends to be a unity, which means that in spite of the considered ductility factor there is a very small reduction in the strength gains by the nonlinear analysis.
- The PGV/PGA ratio has a significant effect on the structural response especially for a long period structure where the response tends to be larger as the PGV/PGA increases.
- Stiff structures with high frequency and short vibration period are insensitive to the variations of the PGV/PGA ratio.
- The most dominate property in case of pulse-like ground motion is the pulse period relative to the structural period. Where the response demand increased as the structural period approaches the pulse period.
- The actual response spectra of a single near-fault earthquake may exceed the elastic spectra of ASCE7 and UBC codes with significant amplification factor. While it can catch the mean response if several records were considered. This is reasonable because most seismic codes produce the shape and the amplitude of the spectrum based on a wide range of data.

## 10. Conflicts of Interest

The authors declare no conflict of interest.

## 11. References

[1] Somerville, P. G., N. F. Smith, R. W. Graves, and N. A. Abrahamson. "Modification of Empirical Strong Ground Motion Attenuation Relations to Include the Amplitude and Duration Effects of Rupture Directivity." Seismological Research Letters 68, no. 1 (January 1, 1997): 199–222. doi:10.1785/gssrl.68.1.199.

[2] Abrahamson N.A., Incorporating effects of near fault tectonic deformation into design ground motions, presentation sponsored by the Earthquake Engineering Research Institute Visiting Professional Program, hosted by the University at Buffalo, 2001.

[3] Chopra, Anil K., and Chatpan Chintanapakdee. "Comparing Response of SDF Systems to Near-Fault and Far-Fault Earthquake Motions in the Context of Spectral Regions." Earthquake Engineering & Structural Dynamics 30, no. 12 (2001): 1769–1789. doi:10.1002/eqe.92.

[4] Alavi, Babak, and Helmut Krawinkler. "Behavior of Moment-Resisting Frame Structures Subjected to Near-Fault Ground Motions." Earthquake Engineering & Structural Dynamics 33, no. 6 (April 15, 2004): 687–706. doi:10.1002/eqe.369.

[5] Heydari, Mahdi, and Mahdi Mousavi. "The Comparison of Seismic Effects of Near-Field and Far-Field Earthquakes on Relative Displacement of Seven-Storey Concrete Building with Shear Wall." Current World Environment 10, no. Special-Issue1 (June 28, 2015): 40–46. doi:10.12944/cwe.10.special-issue1.07.

[6] Alhan, Cenk, and Melih Sürmeli. "Necessity and Adequacy of Near-Source Factors for Not-so-Tall Fixed-Base Buildings." Earthquake Engineering and Engineering Vibration 14, no. 1 (February 20, 2015): 13–26. doi:10.1007/s11803-015-0003-8.

[7] Hosseini, Mahmood, Banafshehalsadat Hashemi, and Zahra Safi. "Seismic Design Evaluation of Reinforced Concrete Buildings for Near-Source Earthquakes by Using Nonlinear Time History Analyses." Procedia Engineering 199 (2017): 176–181. doi:10.1016/j.proeng.2017.09.225.

[8] Talebi Jouneghani, Kourosh, Mahmood Hosseini, Mohammad Sadegh Rohanimanesh, and Morteza Raissi Dehkordi. "Evaluating Main Parameters Effects of Near-Field Earthquakes on the Behavior of Concrete Structures with Moment Frame System." Advances in Science and Technology Research Journal 11, no. 3 (September 3, 2017): 10–23. doi:10.12913/22998624/74135.

[9] Kohrangi, Mohsen, Dimitrios Vamvatsikos, and Paolo Bazzurro. "Pulse-Like Versus Non-Pulse-Like Ground Motion Records: Spectral Shape Comparisons and Record Selection Strategies." Earthquake Engineering & Structural Dynamics 48, no. 1 (September 26, 2018): 46–64. doi:10.1002/eqe.3122.

[10] Pacific Earthquake Engineering Research Center (PEER), Strong Motion Database, http://peer.berkeley.edu Accessed on (September 2018).

[11] California Geological Survey-Strong Motion Instrumentation Program (CGS-SMIP) and (PEER), Technical Report for the PEER Ground Motion Database, beta version, October 2010.

[12] Chopra, Anil K. Dynamics of structures: theory and applications to earthquake engineering. Prentice Hall, 1995. doi:10.1061/(asce)0733-9445(2007)133:5(752).

[13] Liao, Wen-I, Chin-Hsiung Loh, and Shiuan Wan. "Earthquake Responses of RC Moment Frames Subjected to Near-Fault Ground Motions." The Structural Design of Tall Buildings 10, no. 3 (2001): 219–229. doi:10.1002/tal.178.

[14] American Society of Civil Engineers, Minimum Design Loads for Buildings and Other Structures (ASCE/SEI 7-10), 2010.

[15] International Conference of Building Officials, Uniform Building Code, Whittier, California, 1997.